Charmless hadronic B decays and the recent CLEO data

B. Dutta*

Center For Theoretical Physics, Department of Physics, Texas A&M University, College Station, Texas 77843-4242

Sechul Oh[†]

Department of Physics and IPAP, Yonsei University, Seoul 120-749, Korea

In the light of recent experimental data from the CLEO Collaboration we study the decays of B mesons to a pair of pseudoscalar (P) mesons, and a vector (V) meson and a pseudoscalar meson, in the framework of factorization. In order to obtain the best fit for the recent CLEO data, we critically examine the values of several input parameters to which the predictions are sensitive. These input parameters are the form factors, the strange quark mass, $\xi \equiv 1/N_c$ (N_c is the effective number of color), the CKM matrix elements and in particular, the weak phase γ. It is possible to give a satisfactory account of the recent experimental results in $B \rightarrow PP$ and VP decays, with constrained values of a *single* ξ. We identify the decay modes in which CP asymmetries are expected to be large.

I. INTRODUCTION

The CLEO Collaboration [1–5] has recently reported new experimental results on the branching ratios (BRs) of a number of exclusive decay modes where B decays into a pair of pseudoscalars (P), a vector (V) and a pseudoscalar meson, or a pair of vector mesons. Several decay modes have been observed for the first time, such as $B \rightarrow \pi^+ \pi^-$, $K^0 \pi^0$, $\omega \pi^\pm$, $\rho^0 \pi^\pm$, $\rho^\pm \pi^\mp$, $K^{*\pm} \pi^\mp$, and $K^* \eta$. Improved new bounds have been put on the branching ratios for various modes, such as $B \rightarrow K^\pm \pi^\mp$, $K^0 \pi^\pm$, $K^\pm \pi^0$, ωK, $\omega h^\pm$, and $K \eta'$. A search for CP asymmetries in $B \rightarrow K^\pm \pi^\mp$, $K^\pm \pi^0$, $K_S^0 \pi^\pm$, $K \eta'$, and $\omega \pi^\pm$ has also been performed.

Recently, two works have been done to explain the recent CLEO results for B decays: one of them is based on the flavor $SU(3)$ symmetry [6], and the other one involves the framework of factorization [7]. In the latter work, the existence of *two different* effective numbers of color, $N_c^{\text{eff}}(LL)$ and $N_c^{\text{eff}}(LR)$, is essential, and their favored values are $N_c^{\text{eff}}(LL) = 2$ and $N_c^{\text{eff}}(LR) = 6$ to explain the experimental data, except for $\bar{B}^0 \rightarrow K^{*-} \pi^+$ and $\bar{K}^0 \pi^0$.

In the light of the recent CLEO data, in this work, we will analyze *both* $B \rightarrow PP$ and $B \rightarrow VP$ with a *single* parameter ξ in the framework of generalized factorization, in order to find satisfactory explanation compatible with all the recent experimental results. Our approach will be different from that of Ref. [7]. Similar to the case of $B \rightarrow D$ (i.e., heavy $\rightarrow$ heavy) decays, we will assume only one *universal* $\xi \equiv 1/N_c$ (N_c is the effective number of color) in the analysis of both $B \rightarrow PP$ and $B \rightarrow VP$ (P and V are *light* mesons). It has been shown that in $B \rightarrow D$ decays a single ξ can satisfactorily explain experimental data for both $B \rightarrow PP$ (such as $D\pi$) and $B \rightarrow VP$ (such as $D\rho$) [8]. In order to achieve this goal, the values of all the input parameters, e.g., the form factors, the

strange quark mass, N_c, the Cabibbo-Kobayashi-Maskawa (CKM) matrix elements etc., will be carefully examined and constraints on these parameters will be investigated. We shall see that it is indeed possible to account satisfactorily for all the recent experimental data within our framework. In addition, we will discuss CP asymmetries in the B decays and identify the decay modes where the CP asymmetries are possibly large. In our previous works [9,10], we have shown that the predictions for $B \rightarrow PP$ and VP modes are sensitive to several input parameters, such as the form factors, the QCD scale, the parameter $\xi \equiv 1/N_c$, the CKM matrix elements, and the light quark masses, in particular the strange quark mass. With the improved recent data, the results (e.g., $\xi \sim 0$) obtained in the previous works are unlikely to be compatible with the experimental results. Our main emphasis was to explain the large branching ratio for $B \rightarrow K \eta'$ within factorization. In order to explain the large branching ratio for $B \rightarrow K \eta'$, different assumptions have been proposed, e.g., large form factors [11], the QCD anomaly effect [12,13], high charm content in η' [14–16], a new mechanism in the standard model [17], or new physics like supersymmetry without R-parity [18]. In this work we will assume that a certain (unknown) mechanism is (at least in part) responsible for the large branching ratio for $B \rightarrow K \eta'$ and hence will not consider the decay modes having η' in the final states.

We organize this work as follows. In Sec. II we discuss the effective Hamiltonian and obtain the effective Wilson coefficients at the scale m_b for both $b \rightarrow s$ and $b \rightarrow d$ transitions. In Sec. III we describe the parametrization of the matrix elements and define the decay constants and the form factors. In Secs. IV and V the two body decays $B \rightarrow PP$ and $B \rightarrow VP$ are analyzed in the framework of factorization. The CP asymmetries in the B decay modes are also discussed. Finally, in Sec. VI our results are summarized.

II. DETERMINATION OF THE EFFECTIVE WILSON COEFFICIENTS

The effective weak Hamiltonian for hadronic B decays can be written as

———————
*Email address: b-dutta@rainbow.physics.tamu.edu
[†]Email address: scoh@kimcs.yonsei.ac.kr

$$H_{\Delta B=1} = \frac{4G_F}{\sqrt{2}}\left[V_{ub}V_{uq}^*(c_1 O_1^u + c_2 O_2^u) + V_{cb}V_{cq}^*(c_1 O_1^c\right.$$

$$\left. + c_2 O_2^c) - V_{tb}V_{tq}^* \sum_{i=3}^{12} c_i O_i\right] + \text{H.c.}, \qquad (1)$$

where O_i's are defined as

$$O_1^f = \bar{q}\gamma_\mu L f \bar{f}\gamma^\mu L b, \quad O_2^f = \bar{q}_\alpha \gamma_\mu L f_\beta \bar{f}_\beta \gamma^\mu L b_\alpha,$$

$$O_{3(5)} = \bar{q}\gamma_\mu L b \Sigma \bar{q}' \gamma^\mu L(R) q',$$

$$O_{4(6)} = \bar{q}_\alpha \gamma_\mu L b_\beta \Sigma \bar{q}'_\beta \gamma^\mu L(R) q'_\alpha,$$

$$O_{7(9)} = \frac{3}{2}\bar{q}\gamma_\mu L b \Sigma e_{q'} \bar{q}' \gamma^\mu R(L) q',$$

$$O_{8(10)} = \frac{3}{2}\bar{q}_\alpha \gamma_\mu L b_\beta \Sigma e_{q'} \bar{q}'_\beta \gamma^\mu R(L) q'_\alpha,$$

$$O_{11} = \frac{g_s}{32\pi^2} m_b \bar{q}\sigma_{\mu\nu} R T_a b G_a^{\mu\nu},$$

$$O_{12} = \frac{e}{32\pi^2} m_b \bar{q}\sigma_{\mu\nu} R b F^{\mu\nu}, \qquad (2)$$

where $L(R) = (1 \mp \gamma_5)/2$, f can be u or c quark, q can be d or s quark, and q' is summed over u, d, s, and c quarks. α and β are the color indices. T^a is the $SU(3)$ generator with the normalization $\text{Tr}(T^q T^b) = \delta^{ab}/2$. $G_a^{\mu\nu}$ and $F^{\mu\nu}$ are the gluon and photon field strength. c_i's are the Wilson coefficients (WC's). O_1, O_2 are the tree level and QCD corrected operators. O_{3-6} are the gluon induced strong penguin operators. O_{7-10} are the electroweak penguin operators due to γ and Z exchange, and the box diagrams at loop level. In this work we shall take into account the chromomagnetic operator O_{11}, but neglect the extremely small contribution from O_{12}. The dipole contribution is in general quite small, and is of the order of 10% for penguin dominated modes. For all the other modes it can be neglected. The initial values of the WC's are derived from the matching condition at the m_W scale. However we need to renormalize them [19,20] when we use these coefficients at the m_b scale. We will use the effective values of WC's at the scale $\mu = m_b$. It has been shown that in $B \to PP$ case there is very little μ dependence in the final states [9].

We obtain the $c_i(\mu)$'s by solving the following renormalization group equation:

$$\left(-\frac{\partial}{\partial t} + \beta(\alpha_s)\frac{\partial}{\partial\alpha_s}\right)\mathbf{C}(m_W^2/\mu^2, g^2) = \frac{\hat{\gamma}^T(g^2)}{2}\mathbf{C}(t, \alpha_s(\mu), \alpha_e), \qquad (3)$$

where $t \equiv \ln(M_W^2/\mu^2)$ and $\mathbf{C}$ is the column vector that consists of (c_i)'s. The beta and the gamma are given by

$$\beta(\alpha_s) = -\left(11 - \frac{2}{3}n_f\right)\frac{\alpha_s^2}{16\pi^2} - \left(102 - \frac{38}{3}n_f\right)$$

$$\times \frac{\alpha_s^4}{(16\pi^2)^2} + \ldots,$$

$$\hat{\gamma}(\alpha_s) = \left(\gamma_s^{(0)} + \gamma_{se}^{(1)}\frac{\alpha_{em}}{4\pi}\right)\frac{\alpha_s}{4\pi} + \gamma_e^{(0)}\frac{\alpha_{em}}{4\pi}$$

$$+ \gamma_s^{(1)}\frac{\alpha_s^2}{(4\pi)^2} + \ldots, \qquad (4)$$

where α_{em} is the electromagnetic coupling and n_f is the number of active quark flavors.

The anomalous-dimension matrices $\gamma_s^{(0)}$ and $\gamma_e^{(0)}$ determine the leading log corrections and they are renormalization scheme independent. The next to leading order corrections which are determined by $\gamma_{se}^{(1)}$ and $\gamma_s^{(1)}$ are renormalization scheme dependent. The γ's have been determined in Refs. [19,20].

We can express $C(\mu)$ (where μ lies between M_W and m_b) in terms of the initial conditions for the evolution equations

$$C(\mu) = U(\mu, M_W)C(M_W). \qquad (5)$$

$C(M_W)$'s are obtained from matching the full theory to the effective theory at the M_W scale [20,21]. The WC's so far obtained are renormalization scheme dependent. In order to make them scheme independent we need to use a suitable matrix T [20]. The WC's at the scale $\mu = m_b$ are given by

$$\bar{C}(\mu) = TU(m_b, M_W)C(M_W). \qquad (6)$$

The matrix T is given by

$$T = \mathbf{1} + \hat{r}_s^T \frac{\alpha_s}{4\pi} + \hat{r}_e^T \frac{\alpha_e}{4\pi}, \qquad (7)$$

where $\hat{r}$ depends on the number of up-type quarks and the down type quarks, respectively. The r's are given in Ref. [20]. In order to determine the coefficients at the scale $\mu < m_b$, we need to use the matching of the evolutions between the scales larger and smaller than the threshold. In that case, in the expression for T, we need to use $\delta\hat{r}$ instead of $\hat{r}$, where $\delta\hat{r} = r_{u,d} - r_{u,d-1}$ (where u and d are the number of up type quarks and the number of down type quarks, respectively). The matrix elements ($O_i's$) are also needed to have one loop correction. The procedure is to write the one loop matrix element in terms of the tree level matrix element and to generate the effective Wilson coefficients [22]:

$$\langle c_i O_i\rangle = \sum_{ij} c_i(\mu)\left[\delta_{ij} + \frac{\alpha_s}{4\pi}m_{ij}^s + \frac{\alpha_{em}}{4\pi}m_{ij}^e\right]\langle O_j\rangle^{\text{tree}}, \qquad (8)$$

TABLE I. Effective Wilson coefficients for the $b \rightarrow s$ transition at the scales $\mu = m_b$ and $m_b/2$.

WC's	$\mu = m_b$	$\mu = m_b/2$
c_1^{eff}	1.149	1.135
c_2^{eff}	-0.3209	-0.282
c_3^{eff}	$0.02175 - 0.00414i$	$0.0228718 + 0.004689i$
c_4^{eff}	$-0.04906 - 0.01242i$	$-0.051144 - 0.004689i$
c_5^{eff}	$0.01560 + 0.00414i$	$-0.051144 - 0.004689i$
c_6^{eff}	$-0.06063 - 0.01242i$	$-0.0653549 - 0.0140673i$
c_7^{eff}	$-0.000859 + 0.000073i$	$0.00122773 + 0.00005724i$
c_8^{eff}	0.001433	-0.0000953211
c_9^{eff}	$-0.011487 + 0.000073i$	$-0.0120155 + 0.0000572433i$
c_{10}^{eff}	0.003174	0.00218628

$$
\begin{pmatrix}
c_1^{eff} \\
c_2^{eff} \\
c_3^{eff} \\
c_4^{eff} \\
c_5^{eff} \\
c_6^{eff} \\
c_7^{eff} \\
c_8^{eff} \\
c_9^{eff} \\
c_{10}^{eff}
\end{pmatrix}
=
\begin{pmatrix}
\bar{c}_1 \\
\bar{c}_2 \\
\bar{c}_3 - P_s/3 \\
\bar{c}_4 + P_s \\
\bar{c}_5 - P_s/3 \\
\bar{c}_6 + P_s \\
\bar{c}_7 + P_e \\
\bar{c}_8 \\
\bar{c}_9 + P_e \\
\bar{c}_{10}
\end{pmatrix},
\tag{9}
$$

where

$$
P_s = \frac{\alpha_s}{8\pi} \bar{c}_2 \left[\frac{V_{cb}V_{cq}^*}{V_{tb}V_{tq}^*} \left(\frac{10}{9} + G(m_c,\mu,q^2) \right) \right.
$$
$$
\left. + \frac{V_{ub}V_{uq}^*}{V_{tb}V_{tq}^*} \left(\frac{10}{9} + G(m_c,\mu,q^2) \right) \right],
\tag{10}
$$

$$
P_e = \frac{\alpha_{em}}{9\pi} (3\bar{c}_1 + \bar{c}_2) \left[\frac{V_{cb}V_{cq}^*}{V_{tb}V_{tq}^*} \left(\frac{10}{9} + G(m_c,\mu,q^2) \right) \right.
$$
$$
\left. + \frac{V_{ub}V_{uq}^*}{V_{tb}V_{tq}^*} \left(\frac{10}{9} + G(m_c,\mu,q^2) \right) \right].
$$

Here V_{ij} are the elements of the CKM matrix. m_c is the charm quark mass and m_u is the up quark mass. The function $G(m,\mu,q^2)$ is given by

$$
G(m,\mu,q^2) = 4\int_0^1 dx\, x(1-x) \ln \frac{m^2 - x(1-x)q^2}{\mu^2}, \tag{11}
$$

where q is the gluon momenta in the penguin diagram [15,22,26]. In the numerical calculation, we will use $q^2 = m_b^2/2$ which represents the average value and the full expressions for $P_{s,e}$. In Table I we show the values of the

effective Wilson coefficients at the scale m_b and $m_b/2$ for the process $b \rightarrow s q\bar{q}$. Values for $b \rightarrow d q\bar{q}$ can be similarly obtained. These coefficients are scheme independent and gauge invariant.

Since the color octet contribution is neglected in factorization approximation, we keep $\xi \equiv 1/N_c$ as a variable. As an example, let us consider the u quark contribution of the operator O_5 to the process $B^- \rightarrow \pi^0 K^-$. There are two configurations: (part 1) $= \langle K^- | \bar{s}\gamma_\mu(1-\gamma_5)b | B^- \rangle \langle \pi^0 | \bar{u}\gamma_\mu(1+\gamma_5)u | 0 \rangle$. For (part 2), we need to Fierz-transform the operator O_5 to $-2\{(1/N_c)[\bar{u}(1-\gamma_5)b][\bar{s}(1+\gamma_5)u)] + (1/2)[\bar{u}(1-\gamma_5)\lambda_c b][\bar{s}(1+\gamma_5)\lambda_c u]\}$, where λ_c is the color matrix. Only the (part 1) contributes in the factorization approximation. In order to account for this color octet term (part 2), one needs to make ξ a free parameter.

III. HADRONIC MATRIX ELEMENTS IN FACTORIZATION APPROXIMATION

The generalized factorization approximation has been quite successfully used in two body D decays as well as $B \rightarrow D$ decays [8]. The method includes color octet nonfactorizable contribution by treating $\xi \equiv 1/N_c$ as an adjustable parameter [7,9,10,13,15,16,23]. In this work one of our goals is to establish the range of value of a *single* ξ for the best fit in both $B \rightarrow PP$ and VP decays, where P and V are all *light* mesons such as π, $K^{(*)}$, ρ, ω, and ϕ.

Let us describe the parametrizations of the matrix elements and the form factors in the case of $B \rightarrow PP$ and VP decays:

$$
\langle P(p') | V_\mu | B(p) \rangle
$$
$$
= \left[(p'+p)_\mu - \frac{m_B^2 - m_P^2}{q^2} q_\mu \right] F_1(q^2) + \frac{m_B^2 - m_P^2}{q^2} q_\mu F_0(q^2),
\tag{12}
$$

$$
\langle V(\epsilon,p') | (V_\mu - A_\mu) | B(p) \rangle
$$
$$
= \frac{2}{m_B + m_V} i\epsilon_{\mu\nu\alpha\beta} \epsilon^{\nu*} p^\alpha p'^\beta V(q^2) - (m_B + m_V)
$$
$$
\times \left[\epsilon_\mu - \frac{(\epsilon^* \cdot q)}{q^2} q_\mu \right] A_1(q^2) + \frac{(\epsilon^* \cdot q)}{m_B + m_V}
$$
$$
\times \left[(p+p')_\mu - \frac{m_B^2 - m_V^2}{q^2} q_\mu \right] A_2(q^2)
$$
$$
- (\epsilon^* \cdot q) \frac{2m_V}{q^2} q_\mu A_0(q^2),
$$

and the decay constants, f_P and f_V, are given by

$$
\langle 0 | A_\mu | P(p) \rangle = i f_P p_\mu, \quad \langle 0 | V_\mu | V(\epsilon,p) \rangle = i f_V m_V \epsilon_\mu,
\tag{13}
$$

where P, V, V_μ, and A_μ denote a pseudoscalar meson, a vector meson, a vector current, and an axial-vector current,

respectively. $p(p')$ and $m_P(m_V)$ are the momentum of B meson (P or V) and the mass of $P(V)$, respectively. q is given by $q=p-p'$ and ϵ_μ is the polarization vector of V. Note that $F_1(0)=F_0(0)$ and we set $F(q^2=m_P^2)=F(q^2=0)$, since these form factors are assumed to be pole dominated by mesons at scale m_B^2. Among all the form factors in the $\langle V(\epsilon,p')|(V_\mu-A_\mu)|B(p)\rangle$ matrix element, only A_0 survives when we calculate the full $B\to VP$ decay amplitude. The A_0 is related to A_1 and A_2:

$$A_0(0)=\frac{m_B+m_V}{2m_V}A_1(0)-\frac{m_B-m_V}{2m_V}A_2(0). \qquad (14)$$

For our numerical calculations we use the following values of the decay constants (in MeV) [8,10,26]:

$$f_\pi=132, \quad f_K=162, \quad f_\rho=215, \quad f_\omega=215,$$

$$f_{K*}=225, \quad f_\phi=237. \qquad (15)$$

For the values of the form factors, two different sets, based on the Bauer-Stech-Wirbel (BSW) model [24] and light-cone QCD sum rule analysis [25], have been often used in literature [26]. In our analysis, to achieve the best fit, we treat the form factors as parameters in a certain range of values which are reasonably consistent with the frequently used values. We first start with the following values of form factors: $F_0^{B\to\pi}=0.33$, $F_0^{B\to K}=0.38$ obtained in the BSW model, and $A_0^{B\to\rho}=A_0^{B\to\omega}=0.4$. Then, to find the *single* ξ consistently explaining the experimental data, we vary the values of the form factors in a certain range as well as other parameters, such as the CKM weak phase γ and the strange quark mass m_s.

IV. *B* DECAYS INTO TWO PSEUDOSCALARS

Here we consider the decays $B\to\pi\pi$ and $K\pi$. The CLEO collaboration has made first observations of the decay modes $B\to\pi^+\pi^-$ and $K^0\pi^0$, and has presented improved measurement of BRs for $B\to K^\pm\pi^\mp$ and $B^\pm\to K^0\pi^\pm$ and $B^\pm\to K^\pm\pi^0$ as follows [2]:

$$\mathcal{B}(B^0\to\pi^+\pi^-)=(4.3^{+1.6}_{-1.4}\pm0.5)\times10^{-6}, \qquad (16)$$

$$\mathcal{B}(B^0\to K^\pm\pi^\mp)=(17.2^{+2.5}_{-2.4}\pm1.2)\times10^{-6},$$

$$\mathcal{B}(B^\pm\to K^\pm\pi^0)=(11.6^{+3.0+1.4}_{-2.7-1.3})\times10^{-6},$$

$$\mathcal{B}(B^\pm\to K^0\pi^\pm)=(18.2^{+4.6}_{-4.0}\pm1.6)\times10^{-6},$$

$$\mathcal{B}(B^0\to K^0\pi^0)=(14.6^{+5.9+2.4}_{-5.1-3.3})\times10^{-6}.$$

In Figs. 1–5, we plot the BRs averaged over particle-antiparticle decays for the modes $\pi^+\pi^-$, $K^0\pi^\pm$, $K^\pm\pi^\mp$, $K^\pm\pi^0$, and $K^0\pi^0$ in final states as a function of $\xi=1/N_c$ for $\mu=m_b$. In these figures, we use five different kinds of lines corresponding to different values of parameters, in addition to thick solid lines representing the experimental upper and lower bounds. The solid line corresponds to the case of
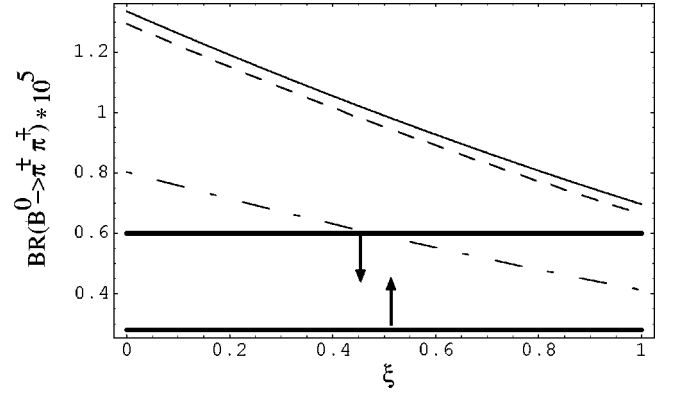

FIG. 1. Branching ratio for $B^0\to\pi^+\pi^-$ as a function of ξ ($\equiv1/N_c$). The solid line: $F_0^{B\to\pi}(0)=0.33$, $F_0^{B\to K}(0)=0.38$, $\gamma=60^0$, and $m_s(m_b)=106$ MeV. The short dashed line: $F_0^{B\to\pi}(0)=0.33$, $F_0^{B\to K}(0)=0.38$, $\gamma=110^0$, and $m_s(m_b)=106$ MeV. The dot-dashed line: $F_0^{B\to\pi}(0)=0.26$, $F_0^{B\to K}(0)=0.29$, $\gamma=110^0$, and $m_s(m_b)=106$ MeV.

choosing the form factors $F_0^{B\to\pi}(0)=0.33$ and $F_0^{B\to K}(0)=0.38$ based on the BSW model, $\gamma\equiv\mathrm{Arg}(V_{ub}^*)=60^0$, $m_s(m_b)=106$ MeV, $V_{cb}=0.040$, $|V_{ub}/V_{cb}|=0.087$, and $|V_{td}|=0.004$. The short dashed line then corresponds to the case of choosing $\gamma=110^0$ and the other parameters are the same as in the solid line case. Similarly, the dot-dash-dot line corresponds to the case of choosing $m_s(m_b)=85$ MeV, while the values of other parameters are the same as in the solid line case. For the dot-dashed and long dashed lines, we choose $m_s(m_b)=106$ MeV and 85 MeV, respectively, with smaller values of form factors $F_0^{B\to\pi}(0)=0.26$ and $F_0^{B\to K}(0)=0.29$, and $\gamma=110^0$. Thus, by comparing each line with the solid line, one can easily see how the decay rate for any mode changes as a particular parameter, such as γ or m_s, changes. Note that in Fig. 1 for $B^0\to\pi^+\pi^-$ decay, the dot-dash-dot and long dashed lines are identical to the solid and dot-dashed lines, respectively, since the amplitude for
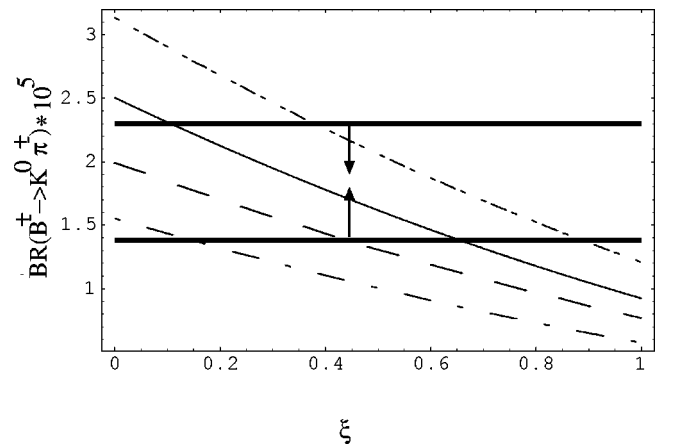

FIG. 2. Branching ratio for $B^\pm\to K^0\pi^\pm$ as a function of ξ ($\equiv1/N_c$). The long dashed line: $F_0^{B\to\pi}(0)=0.26$, $F_0^{B\to K}(0)=0.29$, $\gamma=110^0$, and $m_s(m_b)=85$ MeV. The dot-dash-dot line: $F_0^{B\to\pi}(0)=0.33$, $F_0^{B\to K}(0)=0.38$, $\gamma=60^0$, and $m_s(m_b)=85$ MeV. The definitions for other lines are the same as those in Fig. 1.
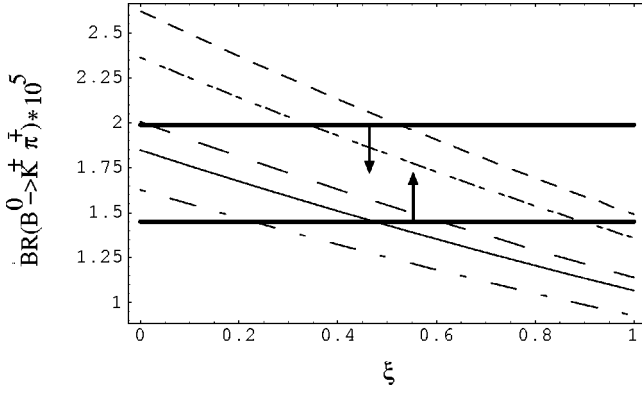
FIG. 3. Branching ratio for $B^0 \to K^\pm \pi^\mp$ as a function of ξ ($\equiv 1/N_c$). The definitions for the lines are the same as those in Figs. 1 and 2.

FIG. 5. Branching ratio for $B^0 \to K^0 \pi^0$ as a function of ξ ($\equiv 1/N_c$). The definitions for the lines are the same as those in Figs. 1 and 2.

this decay mode does not depend on m_s. Similarly, in Fig. 2 for $B^\pm \to K^0 \pi^\pm$ decay, the short dashed line is identical to the solid line since the amplitude for this mode receives contribution from the penguin diagram only and is independent of γ.

The decay rate for $B^0 \to \pi^+ \pi^-$ is proportional to $|F_0^{B \to \pi}|^2$ and is sensitive to the value of the form factor. In Fig. 1, one can see that the BR decreases, as the value of $F_0^{B \to \pi}$ decreases and/or the value of γ increases. In order to fit the experimental upper limit on the BR for this mode, a smaller $F_0^{B \to \pi}$ and a larger γ (dot-dashed line, identical to the long dashed line) are favored. For $F_0^{B \to \pi}(0) = 0.26$ and $\gamma = 110^0$, the values of $\xi \gtrsim 0.44$ are allowed. The rate for $B^\pm \to K^0 \pi^\pm$ is also proportional to $|F_0^{B \to \pi}|^2$ and is sensitive to m_s as well. Figure 2 shows that the BR increases, as the value of $F_0^{B \to \pi}$ increases and/or the value of m_s decreases. In order to find a solution consistent with $B^0 \to \pi^+ \pi^-$, $F_0^{B \to \pi}$ should not be too small and smaller m_s is favored (long dashed line). For $F_0^{B \to \pi}(0) = 0.26$ and $m_s(m_b) = 85$ MeV (long dashed line), the allowed values of ξ are $\xi \lesssim 0.45$. However, for larger $m_s(m_b) = 106$ MeV (dot-dashed line), the allowed values of ξ are smaller $\xi \lesssim 0.15$ and these values of ξ are not allowed by the dot-dashed line for $B^0 \to \pi^+ \pi^-$. In Fig. 3, we plot the
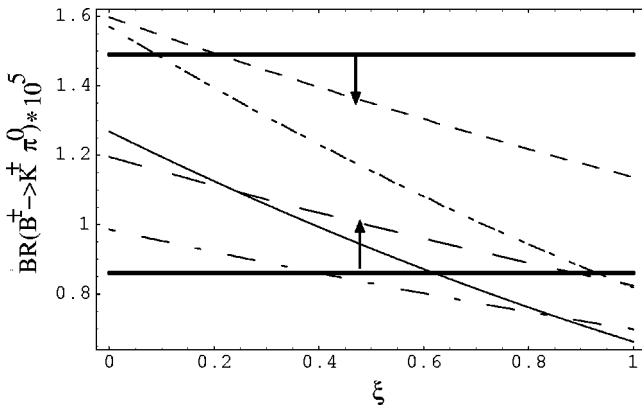

FIG. 4. Branching ratio for $B^\pm \to K^\pm \pi^0$ as a function of ξ ($\equiv 1/N_c$). The definitions for the lines are the same as those in Figs. 1 and 2.
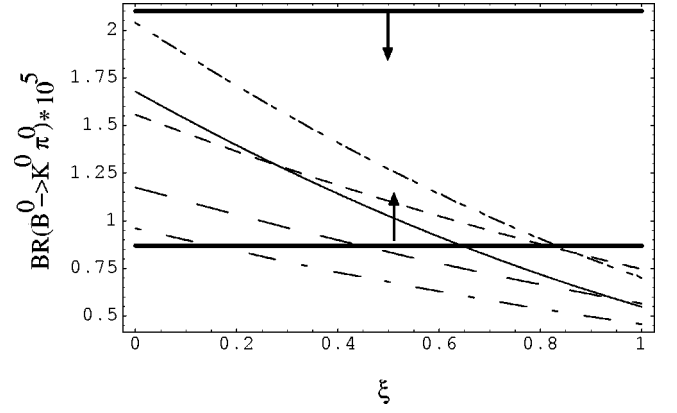
BR for $B^0 \to K^\pm \pi^\mp$ averaged over particle-antiparticle decays as a function of ξ for $\mu = m_b$. This decay mode is sensitive to $F_0^{B \to \pi}$, γ, and m_s. In the case of the long dashed line, the allowed values of ξ are $\xi \lesssim 0.6$, which are consistent with those in $B^0 \to \pi^+ \pi^-$ and $B^+ \to K^0 \pi^+$. Similarly, in Figs. 4 and 5, we plot the BRs for $K^\pm \pi^0$ and $K^0 \pi^0$ in the final states as a function of ξ for $\mu = m_b$. These modes depend on $F_0^{B \to \pi}$, $F_0^{B \to K}$, m_s, and γ. In the long dashed line case, $\xi \lesssim 0.88$ and $\xi \lesssim 0.47$ are allowed for $B \to K^\pm \pi^0$ and $K^0 \pi^0$, respectively, and are consistent with those in the above decays (Figs. 1–3). Therefore, we conclude that the long dashed lines (the dot-dashed line in the case of $B \to \pi^+ \pi^-$) in Figs. 1–5 represent the possible solution compatible with all the experimental limits on the BRs for decay modes $\pi^+ \pi^-$, $K^0 \pi^\pm$, $K^\pm \pi^\mp$, $K^\pm \pi^0$, and $K^0 \pi^0$ in the final states. The values of ξ allowed by the data are those near $\xi \approx 0.45$. (In fact, we shall see that the long dashed line can also consistently explain all the experimental data for $B \to VP$ considered in next section.) Note that the modes $B \to \pi^+ \pi^-$, $K^0 \pi^\pm$, and $K^0 \pi^0$ provide strong constraints on the values of ξ to satisfy the data. In particular, the data on the modes $B \to \pi^+ \pi^-$ and $K^0 \pi^\pm$ put very tight limits on the allowed values of ξ. Hence, an improved measurement of these modes will be important in testing the framework of factorization.

The experimental bounds on the BRs for decays $B \to PP$ provide constraints on the parameters. The favored values of the parameters are

$$F_0^{B \to \pi}(0) = 0.26, \quad F_0^{B \to K}(0) = 0.29, \tag{17}$$

$$\gamma \approx 110^0, \quad m_s(m_b) = 85 \text{ MeV},$$

$$V_{cb} = 0.040, \quad |V_{ub}/V_{cb}| = 0.087, \quad |V_{td}| = 0.004.$$

Current best estimates for CKM matrix elements are $V_{cb} = 0.0381 \pm 0.0021$ and $|V_{ub}/V_{cb}| = 0.085 \pm 0.019$ [27]. The CLEO has recently made the first determination of the value of $\gamma = 113^{0 + 25^0}_{-230}$ by any method other than the unitarity triangle construction [2,28,29]. The favored values for the CKM matrix elements in our analysis above are chosen to

TABLE II. The branching ratios ($\mathcal{B}$) and the CP asymmetries ($\mathcal{A}_{CP}$) for B decay modes into two pseudoscalar mesons at a representative value of $\xi = 0.45$. Charged conjugate modes are implied. The experimental $\mathcal{A}_{CP}$'s represent 90% confidence level intervals.

Decay modes	$\mathcal{B}$ (10^{-6})	Experimental $\mathcal{B}$ (10^{-6})	$\mathcal{A}_{CP}$	Experimental $\mathcal{A}_{CP}$
$B^+ \to \pi^+ \pi^0$	4.38	< 12.7	0	
$B^0 \to \pi^+ \pi^-$	6.00	$4.3^{+1.6}_{-1.4} \pm 0.5$	-0.11	
$B^0 \to K^0 K^+$	0.11	< 5.7	0	
$B^+ \to K^+ \pi^0$	10.14	$11.6^{+3.0+1.4}_{-2.7-1.3}$	-0.061	$[-0.70, 0.16]$
$B^+ \to K^0 \pi^+$	13.34	$18.2^{+4.6}_{-4.0} \pm 1.6$	0	
$B^0 \to K^+ \pi^-$	15.90	$17.2^{+2.5}_{-2.4} \pm 1.2$	-0.066	$[-0.35, 0.27]$
$B^0 \to K^0 \pi^0$	8.70	$14.6^{+5.9+2.4}_{-5.1-3.3}$	-0.01	

get the best fit for the experimental limits on the BRs for the decay processes $B \to PP$ and VP. We find that, if $|V_{ub}|$ increases, the rates for $\pi^+ \pi^-$ and $\omega h (h = \pi, K)$ increase, while the rate for $K^\pm \pi^0$ decreases. Also if $|V_{td}|$ increases, then the rates for $\pi^\pm \pi^\mp$ and $K^\pm \pi^0$ increase and the rate for ωh decreases.

In Table II, we present the BRs and the CP asymmetries for $B \to PP$ decays at a representative value of $\xi = 0.45$. (We shall see that the values of ξ near $\xi \approx 0.45$ are favored to fit all the data.) Available experimental values are also presented. The BRs for all the modes are compatible with the present experimental data. The CP asymmetry, $\mathcal{A}_{CP}$, is defined by

$$\mathcal{A}_{CP} = \frac{\mathcal{B}(b \to f) - \mathcal{B}(\bar{b} \to \bar{f})}{\mathcal{B}(b \to f) + \mathcal{B}(\bar{b} \to \bar{f})}, \tag{18}$$

where b and f denote b quark and a generic final state, respectively. The recent CLEO search for CP asymmetries in $B \to K\pi$ decays has found: $-0.70 \leq \mathcal{A}_{CP}(B^\pm \to K^\pm \pi^0) \leq 0.16$, $-0.35 \leq \mathcal{A}_{CP}(B^0 \to K^\pm \pi^\mp) \leq 0.27$ at 90% confidence limit (C.L.). The expected CP asymmetries in $B \to PP$ decays are generally small and range from -11% to 0.

The BRs in this analysis have been evaluated at the scale m_b. However, if we had chosen the QCD scale $\mu = m_b/2$, the result would not change much [9]. We also see that the favored values of parameters involve a lighter strange quark mass. This, however, is in accordance with the latest trend of lattice results [30]. The ratios of the quark masses are much better known than the individual masses. For example [31],

$$\frac{m_u}{m_d} = 0.553 \pm 0.043; \quad \frac{m_s}{m_d} = 18.9 \pm 0.8. \tag{19}$$

The strange quark mass m_s is in considerable doubt: i.e., QCD sum rules give $m_s(1 \text{ GeV}) = (175 \pm 25)$ MeV and lattice gauge theory gives $m_s(2 \text{ GeV}) = (100 \pm 20 \pm 10)$ MeV in the quenched lattice calculation [31]. In this analysis we have varied m_s from 150 to 116 MeV at 1 GeV scale. We see that the m_s of 116 MeV gives rise to the best fit. We have

used the quark masses at the m_b scale. The magnitude of m_s reduces from 150 to 106 MeV and from 116 to 85 MeV at the m_b scale through 3 loop QCD and 1 loop QED RGEs. The magnitudes of the other quark masses (m_u and m_d) also depend on the strange quark mass. Satisfying the constraints from Eq. (19), the values of m_d we have used are 5.9 MeV (corresponding to $m_s = 150$ MeV) and 4.7 MeV (corresponding to $m_s = 116$ MeV) at the m_b scale. Similarly, the values of m_u we have used are 3.4 MeV (corresponding to $m_s = 150$ MeV) and 2.8 MeV (corresponding to $m_s = 116$ MeV) at the m_b scale.

The difference in m_s affects the BRs for the $B \to \pi K$ modes, since the amplitudes contain a factor such as $X = M_K^2/((m_b + m_u)(m_s + m_u))$. On the other hand, changes in m_d or m_u do not affect the BRs significantly. In the case of $|\Delta S| = 1$ decays, m_u or m_d can always be neglected compared to m_b or m_s in the factor X. In the case of $\Delta S = 0$ decays, the tree contribution is large compared to the penguin contribution and the factor similar to X appears only in the penguin term. Hence the effect is small. For example, the BR for $B^0 \to \pi^+ \pi^-$ changes from 6.00×10^{-6} to 6.10×10^{-6} at $\xi = 0.45$, when one changes the m_d from 5.9 MeV to 4.7 MeV (changing the m_u mass as well). Similar results hold true also in the $B \to VP$ case.

V. B DECAYS INTO A VECTOR AND A PSEUDOSCALAR

We now analyze the decay processes $B \to VP$ which include $B \to \omega \pi(K)$, $\rho \pi(K)$, $\phi \pi(K)$, and $K^* \pi(K)$. The recent measurement at CLEO has yielded the following bounds [5]:

$$\mathcal{B}(B^\pm \to \omega \pi^\pm) = (11.3^{+3.3}_{-2.9} \pm 1.4) \times 10^{-6}, \tag{20}$$

$$\mathcal{B}(B^\pm \to \omega h^\pm) = (14.3^{+3.6}_{-3.2} \pm 2.0) \times 10^{-6},$$

$$\mathcal{B}(B^\pm \to \rho^0 \pi^\pm) = (10.4^{+3.3}_{-3.4} \pm 2.1) \times 10^{-6},$$

$$\mathcal{B}(B^0 \to \rho^\pm \pi^\mp) = (27.6^{+8.4}_{-7.4} \pm 4.2) \times 10^{-6},$$

$$\mathcal{B}(B^0 \to K^{*\pm} \pi^\mp) = (22^{+8+4}_{-6-5}) \times 10^{-6},$$

and

$$\mathcal{B}(B^\pm \to \omega K^\pm) < 7.9 \times 10^{-6}, \tag{21}$$

$$\mathcal{B}(B^\pm \to \phi K^\pm) = (6.4^{+2.5+0.5}_{-2.1-2.0}) \times 10^{-6},$$

where $h^\pm$ denotes $\pi^\pm$ or $K^\pm$, and the BR for $B^0 \to \rho^\pm \pi^\mp$ is the sum of the BRs for $B^0 \to \rho^+ \pi^-$ and $B^0 \to \rho^- \pi^+$. Note that the above BR for $B^0 \to K^{*\pm} \pi^\mp$ still involves a large error.

As in the case of $B \to PP$ decays, in Figs. 6–11, we plot the BRs averaged over particle-antiparticle decays for the modes $B \to \omega \pi^\pm$, $\omega h^\pm$, $\omega K^\pm$, $\rho^\pm \pi^\mp$, $\phi K^\pm$, and $K^{*\pm} \pi^\mp$ as a function of ξ for $\mu = m_b$. Six different kinds of lines are used, corresponding to different values of parameters. The definitions of the (five) lines are the same as those in B
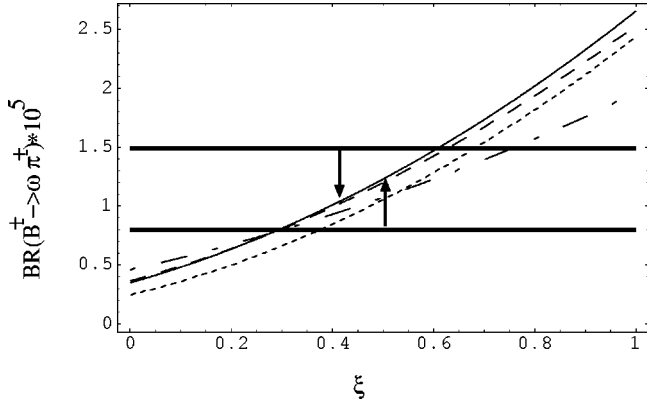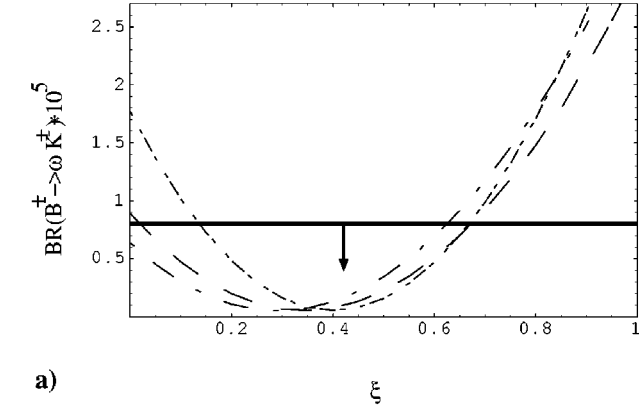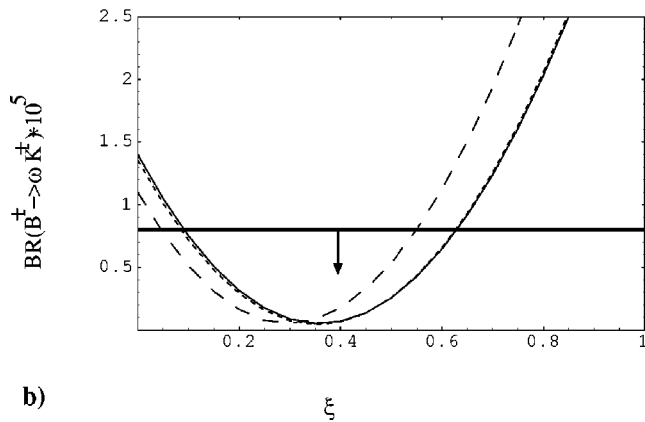
FIG. 6. Branching ratio for $B^{\pm} \to \omega \pi^{\pm}$ as a function of ξ ($\equiv 1/N_c$). The solid line: $F_0^{B \to \pi}(0) = 0.33$, $F_0^{B \to K}(0) = 0.38$, $\gamma = 60^0$, $A_0(0) = 0.4$, and $m_s(m_b) = 106$ MeV. The short dashed line: $F_0^{B \to \pi}(0) = 0.33$, $F_0^{B \to K}(0) = 0.38$, $\gamma = 110^0$, $A_0(0) = 0.4$, and $m_s(m_b) = 106$ MeV. The dotted line: $F_0^{B \to \pi}(0) = 0.33$, $F_0^{B \to K}(0) = 0.38$, $\gamma = 60^0$, $A_0(0) = 0.36$, and $m_s(m_b) = 106$ MeV. The dot-dashed line: $F_0^{B \to \pi}(0) = 0.26$, $F_0^{B \to K}(0) = 0.29$, $\gamma = 110^0$, $A_0(0) = 0.4$, and $m_s(m_b) = 106$ MeV.
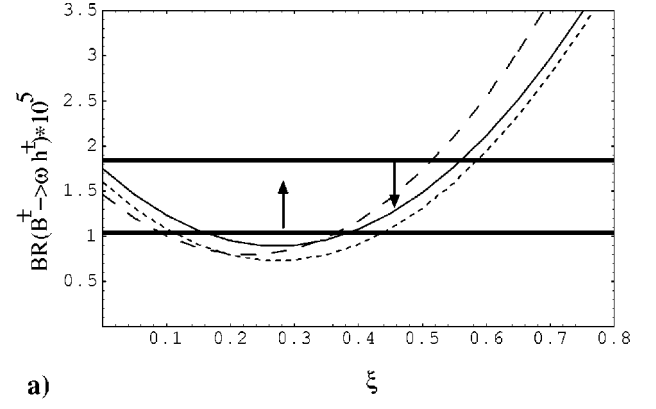

a)
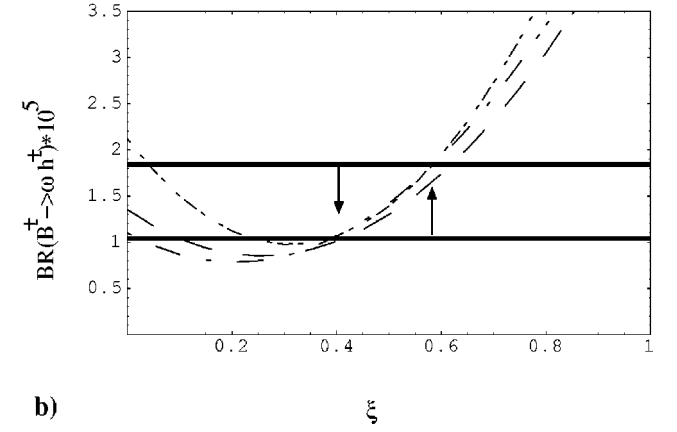

b)

FIG. 7. Branching ratio for $B^{\pm} \to \omega K^{\pm}$ as a function of ξ ($\equiv 1/N_c$). The long dashed line: $F_0^{B \to \pi}(0) = 0.26$, $F_0^{B \to K}(0) = 0.29$, $\gamma = 110^0$, $A_0(0) = 0.4$, and $m_s(m_b) = 85$ MeV. The dot-dashed-dot line: $F_0^{B \to \pi}(0) = 0.33$, $F_0^{B \to K}(0) = 0.38$, $\gamma = 60^0$, $A_0(0) = 0.4$, and $m_s(m_b) = 85$ MeV. The definitions for other lines are the same as those in Fig. 6.

a)

b)

FIG. 8. Branching ratio for $B^{\pm} \to \omega h^{\pm}$ as a function of ξ ($\equiv 1/N_c$). The definitions for the lines are the same as those in Figs. 6 and 7.

$\to PP$ case, except that the form factors $A_0(0) \equiv A_0^{B \to \rho}(0)$ $= A_0^{B \to \omega}(0) = 0.4$ are now added. The dotted line is newly introduced, which corresponds to $A_0(0) = 0.36$ with the same values of other parameters as those in the solid line case. Thus, a comparison of the dotted line with the solid line shows how the BR for a particular mode changes as A_0 changes.
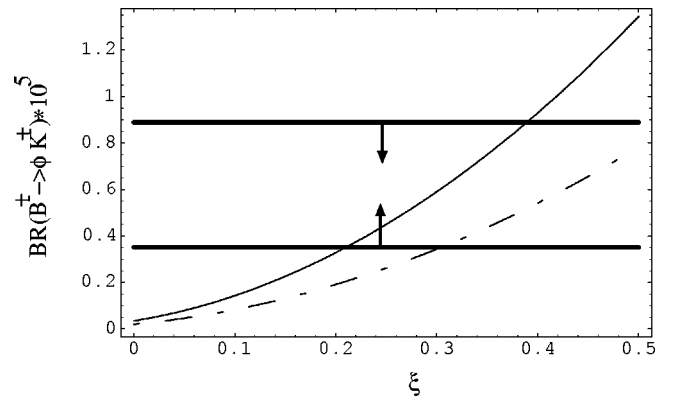

FIG. 9. Branching ratio for $B^{\pm} \to \phi K^{\pm}$ as a function of ξ ($\equiv 1/N_c$). The definitions for the lines are the same as those in Figs. 6 and 7.

a)

b)

FIG. 10. Branching ratios for $B^0 \to \rho^\pm \pi^\mp$ and $B^\pm \to \rho^0 \pi^\pm$ as a function of $\xi (\equiv 1/N_c)$. The definitions for the lines are the same as those in Figs. 6 and 7.

In Fig. 6, we present the plot of the BR for $B^\pm \to \omega \pi^\pm$ as a function of ξ. This decay mode receives the dominant contribution from the tree diagram and is sensitive to the form factors $A_0^{B \to \omega}$, $F_1^{B \to \pi}$, and the weak phase γ. The long dashed line and the dot-dash-dot line are identical to the dot-dashed line and the solid line, respectively, since the rate for this mode does not depend on m_s. All the lines are well within the experimental limits for values of ξ in a broad region. In the case of the long dashed line, the allowed val-

FIG. 11. Branching ratio for $B^0 \to K^{*\pm} \pi^\mp$ as a function of ξ ($\equiv 1/N_c$). The definitions for the lines are the same as those in Figs. 6 and 7.
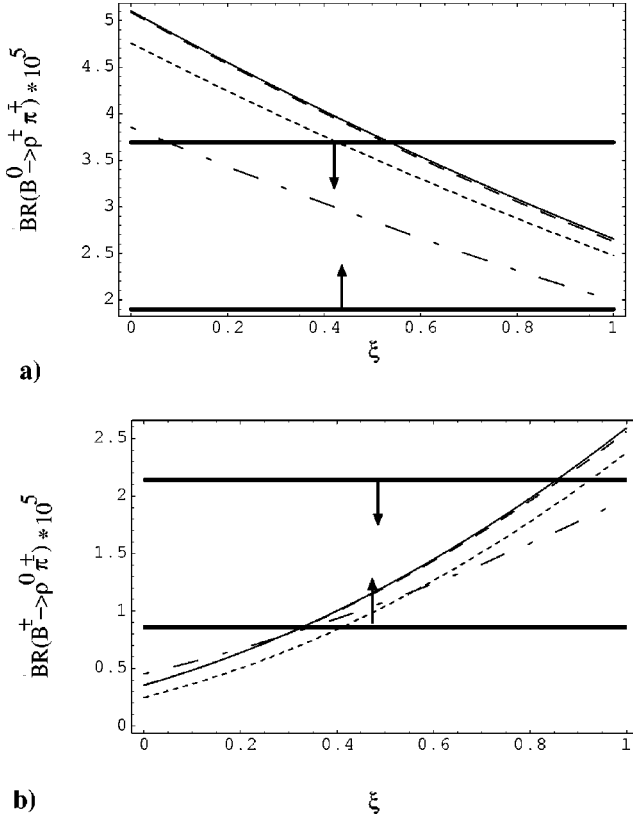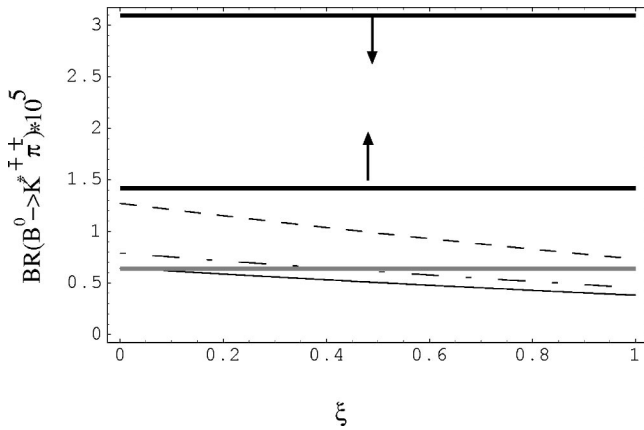
ues of ξ are $0.3 \lesssim \xi \lesssim 0.75$. The recent CLEO search for CP asymmetry in $B^\pm \to \omega \pi^\pm$ decay has found: $-0.80 \leqslant \mathcal{A}_{CP}(B^\pm \to \omega \pi^\pm) \leqslant 0.12$ at 90% C.L. We find that the expected CP asymmetry in this mode is -11% for a representative value of $\xi = 0.45$ (we shall see below that the values of ξ near $\xi \approx 0.45$ are the favored values for the best fit).

The plot of the BR for $B^\pm \to \omega K^\pm$ as a function of ξ is shown in Fig. 7. The rate for this process depends on $A_0^{B \to \omega}$, $F_1^{B \to K}$, γ, and m_s. The previous experimental result from CLEO for this decay mode [32] showed the large BR of $\mathcal{B}(B^\pm \to \omega K^\pm) = (15^{+7}_{-6} \pm 2) \times 10^{-6}$, but in the recent CLEO report [5] the statistical significance for this mode is only 2.1σ and the upper limit for the BR at 90% C.L. has been set as in Eq. (21), which is much lower than the previous one. Thus, as can be seen in Fig. 7, the values of ξ in a broad region are compatible with the experimental upper limit. However, in our earlier work [10], only smaller values of $\xi \lesssim 0.05$ or larger values of $\xi > 0.6$ were allowed to fit the previous data. The allowed values of ξ for the long dashed line are $\xi \lesssim 0.67$. At a representative value of $\xi = 0.45$, the expected BR for this mode is $\mathcal{B}(B^\pm \to \omega K^\pm) = 1.33 \times 10^{-6}$.

Figure 8 shows the plot of the BR for $B^\pm \to \omega h^\pm$ as a function of ξ, where h is π or K. To obtain the best fit for this mode, smaller values of $F_1^{B \to \pi}$, $F_1^{B \to K}$, and γ, and larger values of $A_0^{B \to \omega}$ and m_s are favored. The previous CLEO measurement of the BR for this mode [32] was $\mathcal{B}(B^\pm \to \omega h^\pm) = (25^{+8}_{-7} \pm 3) \times 10^{-6}$, but the recent value [5] has been reduced to $\mathcal{B}(B^\pm \to \omega h^\pm) = (14.3^{+3.6}_{-3.2} \pm 2.0) \times 10^{-6}$. Thus, the values of $\xi \lesssim 0.1$ and $0.4 \lesssim \xi \lesssim 0.64$ for the long dashed line are compatible with the recent data in this mode, while the previous allowed values of ξ are $\xi \approx 0$ and $\xi \gtrsim 0.5$. The expected BR for this mode at a representative value of $\xi = 0.45$ is $\mathcal{B}(B^\pm \to \omega h^\pm) = 11.34 \times 10^{-6}$.

The case of $B^\pm \to \phi K^\pm$ is shown in Fig. 9. The previous CLEO result for this mode [32] was $\mathcal{B}(B^\pm \to \phi K^\pm) < 5 \times 10^{-6}$ at 90% C.L. but recently CLEO has announced the new data [5]: $\mathcal{B}(B^\pm \to \phi K^\pm) = (6.4^{+2.5+0.5}_{-2.1-2.0}) \times 10^{-6}$, $\mathcal{B}(B^0 \to \phi K_S^0) < 12 \times 10^{-6}$, and the combined branching ratio $\mathcal{B}(B \to \phi K) = (6.2^{+2.0+0.7}_{-1.8-1.7}) \times 10^{-6}$. [The Belle Collaboration has recently reported the branching ratio [5]: $\mathcal{B}(B^\pm \to \phi K^\pm) = (17.2^{+6.7}_{-5.4} \pm 1.8) \times 10^{-6}$, which is very large and inconsistent with the CLEO data. To be consistent, in this analysis we use the recent CLEO data only. Future improved data for this mode are called for.] This decay is a pure penguin process and is sensitive to $F_1^{B \to K}$, but independent of A_0, γ, and m_s. A smaller $F_1^{B \to K}$ is favored for a better fit in this decay. But the decays $B \to K\pi$ disfavor too small values of $F_{0,1}^{B \to \pi}$ and $F_{0,1}^{B \to K}$. We find that $F_0^{B \to \pi}(0) \approx 0.26$, $F_0^{B \to K}(0) \approx 0.29$ are favored. For the dot-dashed line, identical to the long dashed line in this mode, the values of $0.3 \lesssim \xi \lesssim 0.55$ are compatible with the data.

In Fig. 10, we present the cases of $B \to \rho \pi$ decays in which the tree contribution is dominant. In (a), the sum of the BRs for $B^0 \to \rho^+ \pi^-$ and $B^0 \to \rho^- \pi^+$ as a function of ξ is shown in order to compare with the recent CLEO data in Eq. (20). The decay $B^0 \to \rho^+ \pi^-$ is sensitive to $F_1^{B \to \pi}$ and γ, while $B^0 \to \rho^- \pi^+$ is sensitive to $A_0^{B \to \rho}$ and γ. The lines are

TABLE III. The branching ratios ($\mathcal{B}$) and the *CP* asymmetries ($\mathcal{A}_{CP}$) for *B* decay modes ($\Delta S = 0$) into a vector and a pseudoscalar meson at a representative value of $\xi = 0.45$. Charged conjugate modes are implied. The experimental branching ratio with $\dagger$ below is the sum of $B^0 \to \rho^+ \pi^-$ and $\rho^- \pi^+$. The experimental $\mathcal{A}_{CP}$ represents a 90% confidence level interval.

Decay modes	$\mathcal{B}$ (10^{-6})	Experimental $\mathcal{B}$ (10^{-6})	$\mathcal{A}_{CP}$	Experimental $\mathcal{A}_{CP}$
$B^+ \to \omega \pi^+$	10.01	$11.3^{+3.3}_{-2.9} \pm 1.4$	-0.11	$[-0.80, 0.12]$
$B^+ \to \rho^0 \pi^+$	10.06	$10.4^{+3.3}_{-3.4} \pm 2.1$	0.047	
$B^+ \to \rho^+ \pi^0$	10.51	<43	-0.039	
$B^+ \to \bar{K}^{*0} K^+$	0.043	<5.3	0	
$B^+ \to K^{*+} \bar{K}^0$	0.013		0	
$B^+ \to \phi \pi^+$	0.0028	<4.0	0	
$B^0 \to \omega \pi^0$	0.032	<5.5	-0.18	
$B^0 \to \rho^+ \pi^-$	15.39	$27.6^{+8.4}_{-7.4} \pm 4.2^{\dagger}$	-0.072	
$B^0 \to \rho^- \pi^+$	14.02		-0.015	
$B^0 \to \rho^0 \pi^0$	0.65	<5.5	-0.27	
$B^0 \to K^{*0} \bar{K}^0$	0.13		0	
$B^0 \to \phi \pi^0$	0.0014	<5.4	0	

TABLE IV. The branching ratios ($\mathcal{B}$) and the *CP* asymmetries ($\mathcal{A}_{CP}$) for *B* decay modes ($|\Delta S| = 1$) into a vector and a pseudoscalar meson at a representative value of $\xi = 0.45$. Charged conjugate modes are implied. The experimental branching ratio with * below is from Ref. [33].

Decay modes	$\mathcal{B}$ (10^{-6})	Experimental $\mathcal{B}$ (10^{-6})	$\mathcal{A}_{CP}$
$B^+ \to \omega K^+$	1.33	<7.9	-0.19
$B^+ \to \rho^0 K^+$	0.67	<17	0.13
$B^+ \to \rho^- K^0$	1.20	$<48*$	0
$B^+ \to K^{*0} \pi^+$	4.06	<16	0
$B^+ \to K^{*+} \pi^0$	3.56	<31	0.15
$B^+ \to \phi K^+$	6.56	$6.4^{+2.5+0.5}_{-2.1-2.0}$	0
$B^0 \to \omega K^0$	0.15	<21	-0.29
$B^0 \to \rho^- K^+$	1.28	<32	0.10
$B^0 \to \rho^0 K^0$	0.082	<27	0.17
$B^0 \to K^{*0} \pi^0$	0.76	<3.6	-0.13
$B^0 \to K^{*+} \pi^-$	6.27	22^{+8+4}_{-6-5}	-0.14
$B^0 \to \phi K^0$	6.56	<12	0

well within the experimental upper and lower limits for most values of ξ. For the dot-dashed line, identical to the long dashed line, the allowed values of ξ are $\xi \gtrsim 0.08$. The expected BR for this mode is $\mathcal{B}(B^0 \to \rho^{\pm} \pi^{\mp}) = 29.41 \times 10^{-6}$ at a representative value of $\xi = 0.45$. The case of $B^{\pm} \to \rho^0 \pi^{\pm}$ is shown in (b). This process is sensitive to $A_0^{B \to \rho}$, $F_1^{B \to \pi}$, and γ. For the dot-dashed line, identical to the long dashed line, the values of $\xi \gtrsim 0.34$ are compatible with the experimental data. This can be compared with the case of $B^{\pm} \to \omega \pi^{\pm}$ shown in Fig. 6. These two modes are both tree-dominated and have similar values of masses, decay constants, and form factors. So it is expected that their BRs are not very different: the recent CLEO data for $\rho^0 \pi^{\pm}$ and $\omega \pi^{\pm}$ decays are $(10.4^{+3.3}_{-3.4} \pm 2.1) \times 10^{-6}$ and $(11.3^{+3.3}_{-2.9} \pm 1.4) \times 10^{-6}$, respectively, as in Eq. (20). The favored values in our analysis are $\mathcal{B}(B^{\pm} \to \rho^0 \pi^{\pm}) = 10.06 \times 10^{-6}$ and $\mathcal{B}(B^{\pm} \to \omega \pi^{\pm}) = 10.01 \times 10^{-6}$ at a representative value of $\xi = 0.45$, which are consistent with the recent data.

Figure 11 shows the plot of $\mathcal{B}(B^0 \to K^{*\pm} \pi^{\mp})$ as a function of ξ. This mode receives the dominant contribution from the penguin diagram. Our theoretical expectation of the BR for this decay is less than the experimental limits at 1σ level (thick lines), but is greater than the lower limit at 2σ level (gray line). Thus, within 2σ range, our result is compatible with the data for this mode. Since the measurement of this decay still involves large error, an improvement in the experiment will be crucial to test the framework of our work.

In Tables III and IV, we present the BRs and the *CP* asymmetries for the decays $B \to VP (\Delta S = 0$ and $|\Delta S| = 1)$ at a representative value of $\xi = 0.45$. Available experimental results are also presented. All the theoretical values are compatible with the present experimental bounds. In particular, in some decay modes, the *CP* asymmetries are expected to be large. Among $\Delta S = 0$ decays, the *CP* asymmetry is ex-

pected to be relatively large in a few decay modes: (i) in $B^0 \to \rho^0 \pi^0$, the expected *CP* asymmetry is -27% with the expected BR of 0.65×10^{-6}, (ii) in $B^0 \to \omega \pi^0$, the *CP* asymmetry is expected to be -18% with the expected BR of 0.032×10^{-6}, (iii) in $B^{\pm} \to \omega \pi^{\pm}$, the *CP* asymmetry is expected to be -11% with the expected BR of 10.01×10^{-6}. Among $|\Delta S| = 1$ decays, there are several interesting modes: (i) the expected *CP* asymmetry in $B^0 \to \omega K^0$ is -29% with the expected BR of 0.15×10^{-6}, (ii) the expected *CP* asymmetry in $B^{\pm} \to \omega K^{\pm}$ is -19% with the expected BR of 1.33×10^{-6}, (iii) the *CP* asymmetry in $B^0 \to K^{*\pm} \pi^{\mp}$ is expected to be -14% with the expected BR of 6.27×10^{-6}, (iv) the *CP* asymmetry in $B^{\pm} \to K^{*\pm} \pi^0$ is expected to be 15% with the expected BR of 3.56×10^{-6}.

VI. CONCLUSION

Motivated by the recent CLEO data, we have analyzed charmless hadronic two body decays of *B* mesons $B \to PP$ and $B \to VP$. In the framework of generalized factorization, we have carefully examined the values of several input parameters to which the predictions are sensitive. Those input parameters are the form factors, the strange quark mass, $\xi \equiv 1/N_c$, the CKM matrix elements, and in particular, the weak phase γ.

We have found that the experimental bounds on the BRs for the decay modes $B \to \pi^+ \pi^-$, $K^0 \pi^{\pm}$, and $K^0 \pi^0$ among $B \to PP$ modes put strong constraints on the parameters. The constraints on parameters from the decays $B^{\pm} \to \omega h^{\pm}$ among $B \to VP$ are also strong and lead to the following favored values of the parameters for the best fit [in Figs. 1–11, the long dashed line (or the dot-dashed line when the long dashed line is absent) represents the case corresponding to the best fit]:

$$\xi \approx 0.45 \tag{22}$$

$$F_0^{B \to \pi}(0) = 0.26, \quad F_0^{B \to K}(0) = 0.29,$$

$$A_0^{B \to \rho}(0) = 0.4, \quad A_0^{B \to \omega}(0) = 0.4,$$

$$\gamma \approx 110^0, \quad m_s(m_b) = 85 \text{ MeV},$$

$$V_{cb} = 0.040, \quad |V_{ub}/V_{cb}| = 0.087, \quad |V_{td}| = 0.004.$$

[In fact, a little smaller values of $A_0(0)$ are also allowed.] It has been known that there exists the discrepancy in values of γ extracted from the CKM-fitting at $\rho - \eta$ plan [34] and from the χ^2 analysis of hadronic decays of B mesons [29]. The value of γ obtained from the each case is $\gamma = 60°$ $\sim 80°$ from the CKM-fitting at $\rho - \eta$ plane, or $\gamma = 90°$ $\sim 140°$ from the hadronic B decay analysis. In our analysis we find that $\gamma \approx 110°$ is favored to fit the given data. We have shown that the recent CLEO data in $B \to PP$ and VP modes can be satisfactorily explained with $\xi \approx 0.45$, except for the BR of the decay mode $B^0 \to K^{*\pm} \pi^{\mp}$ at 1σ level [at 2σ level, our prediction for $\mathcal{B}(B^0 \to K^{*\pm} \pi^{\mp})$ is compatible with the data]. An improved measurement of the BR for this process will be crucial in testing the framework of factorization. We have also identified the decay modes where the CP asymmetries are expected to be large, such as $B \to \rho^0 \pi^0$, $\omega \pi^0$, $\omega \pi^{\pm}$ in $\Delta S = 0$ decays, and $B \to \omega K^0$, $\omega K^{\pm}$, $K^{*\pm} \pi^0$, $\rho^0 K^0$ in $|\Delta S| = 1$ decays.

[1] CLEO Collaboration, Y. Gao and F. Würthwein, CALT 68-2220, HUTP-99/A021, hep-ex/9904008.

[2] CLEO Collaboration, D. Cronin-Hennessy *et al.*, Phys. Rev. Lett. **85**, 515 (2000); CLEO Collaboration, Y. Kwon *et al.*, CLEO CONF 99-14, hep-ex/9908039.

[3] CLEO Collaboration, S. J. Richichi *et al.*, Phys. Rev. Lett. **85**, 520 (2000).

[4] CLEO Collaboration, T. E. Coan *et al.*, CLEO CONF 99-16, hep-ex/9908029.

[5] CLEO Collaboration, D. Cinabro, hep-ex/0009045; Belle Collaboration, P. Chang, talk presented at XXXth International Conference on High Energy Physics, Osaka, Japan, 2000; CLEO Collaboration, C. P. Jessop *et al.*, Phys. Rev. Lett. **85**, 2881 (2000); CLEO Collaboration, M. Bishai *et al.*, CLEO CONF 99-13, hep-ex/9908018; CLEO Collaboration, J. G. Smith, invited talk presented at the Third International Conference on B Physics and CP Violation, Taipei, Taiwan, 1999.

[6] M. Gronau and J. L. Rosner, Phys. Rev. D **61**, 073008 (2000).

[7] H.-Y. Cheng and K.-C. Yang, Phys. Rev. D **62**, 054029 (2000).

[8] M. Neubert and B. Stech, in *Heavy Flavors*, 2nd ed., edited by A. J. Buras and M. Linder (World Scientific, Singapore), hep-ph/9705292.

[9] N. G. Deshpande, B. Dutta, and Sechul Oh, Phys. Rev. D **57**, 5723 (1998).

[10] N. G. Deshpande, B. Dutta, and Sechul Oh, Phys. Lett. B **473**, 141 (2000).

[11] A. L. Kagan and A. A. Petrov, UCHEP-27, UMHEP-443, hep-ph/9707354; A. Datta, X.-G. He, and S. Pakvasa, Phys. Lett. B **419**, 369 (1998).

[12] D. Atwood and A. Soni, Phys. Lett. B **405**, 150 (1997); W.-S. Hou and B. Tseng, Phys. Rev. Lett. **80**, 434 (1998).

[13] A. Ali, J. Chay, C. Greub, and P. Ko, Phys. Lett. B **424**, 161 (1998).

[14] I. Halperin and A. Zhitnitsky, Phys. Rev. Lett. **80**, 438 (1998).

[15] A. Ali and C. Greub, Phys. Rev. D **57**, 2996 (1998), and references therein.

[16] H.-Y. Cheng and B. Tseng, Phys. Lett. B **415**, 263 (1997).

[17] D. Du, C. S. Kim, and Y. Yang, Phys. Lett. B **426**, 133 (1998); M. R. Ahmady, E. Kou, and A. Sugamoto, Phys. Rev. D **58**, 014015 (1998).

[18] D. Choudhury, B. Dutta, and Anirban Kundu, Phys. Lett. B **456**, 185 (1999).

[19] A. J. Buras, M. Jamin, M. E. Lautenbacher, and P. Weisz, Nucl. Phys. **B400**, 37 (1993); A. J. Buras, M. Jamin, and M. E. Lautenbacher, *ibid.* **B400**, 75 (1993).

[20] M. Ciuchini, E. Franco, G. Martinelli, and L. Reina, Nucl. Phys. **B415**, 403 (1994).

[21] A. J. Buras, M. Jamin, and M. E. Lautenbacher, Nucl. Phys. **B370**, 69 (1992).

[22] R. Fleischer, Z. Phys. C **62**, 81 (1994); **58**, 483 (1993); G. Kramer, W. Palmer, and H. Simma, Nucl. Phys. **B428**, 77 (1994).

[23] N. G. Deshpande, M. Gronau, and D. Sutherland, Phys. Lett. **90B**, 431 (1980); M. Neubert, Nucl. Phys. B (Proc. Suppl.) **64**, 474 (1998); B. Stech, Plenary talk given at 20th Anniversary Symposium: Twenty Beautiful Years of Bottom Physics, Chicago, Illinois, hep-ph/9709280.

[24] M. Bauer and B. Stech, Phys. Lett. **152B**, 380 (1985); M. Bauer, B. Stech, and M. Wirbel, Z. Phys. C **34**, 103 (1987).

[25] P. Ball and V. M. Braun, Phys. Rev. D **58**, 094016 (1998); P. Ball, J. High Energy Phys. **09**, 005 (1998).

[26] A. Ali, G. Kramer, and C.-D. Lü, Phys. Rev. D **58**, 094009 (1998); Y.-H. Chen, H.-Y. Cheng, B. Tseng, and K.-C. Yang, *ibid.* **60**, 094014 (1999), and references therein.

[27] S. Stone, presented at Heavy Flavours 8, Southampton, UK, July 1999, hep-ph/9910417.

[28] W.-S. Hou, J. G. Smith, and F. Würthwein, NTUHEP-99-25, COLO-HEP-438, LNS-99-290, hep-ex/9910014.

[29] Also see N. G. Deshpande, X.-G. He, W.-S. Hou, and S. Pakvasa, Phys. Rev. Lett. **82**, 2240 (1999); X.-G. He, W.-S. Hou, and K.-C. Yang, *ibid.* **83**, 1100 (1999).

[30] S. Ryan, Fermilab Conf-99/222-T, hep-ph/9908386.

[31] H. Leutwyler, Phys. Lett. B **374**, 163 (1996).

[32] CLEO Collaboration, M. S. Alam *et al.*, CLEO CONF 97-23; CLEO Collaboration, A. Anastassov *et al.*, CLEO CONF 97-24.

[33] CLEO Collaboration, presented by J. G. Smith at the 1997 Aspen Winter Conference on Particle Physics, Aspen, Colorado, 1997; D. M. Asner *et al.*, Phys. Rev. D **53**, 1039 (1996); K. Lingel, T. Skwarnicki, and J. G. Smith, Annu. Rev. Nucl. Part. Sci. **48**, 253 (1998).

[34] F. Caravaglios *et al.*, LAL 00-04, hep-ph/0002171.